World Academy of Science, Engineering and Technology
International Journal of Pharmacological and Pharmaceutical Sciences
Vol:8, No:7, 2014

Preparation and *in vivo* Assessment of Nystatin-Loaded Solid Lipid Nanoparticles for Topical Delivery against Cutaneous Candidiasis

Rawia M. Khalil, Ahmed A. Abd El Rahman, Mahfouz A. Kassem, Mohamed S. El Ridi, Mona M. Abou Samra, Ghada E. A. Awad, Soheir S. Mansy

Open Science Index, Pharmacological and Pharmaceutical Sciences Vol:8, No:7, 2014 publications.waset.org/9999007.pdf

***Abstract*—**Solid lipid nanoparticles (SLNs) have gained great attention for the topical treatment of skin associated fungal infection as they facilitate the skin penetration of loaded drugs. Our work deals with the preparation of nystatin loaded solid lipid nanoparticles (NystSLNs) using the hot homogenization and ultrasonication method. The prepared NystSLNs were characterized in terms of entrapment efficiency, particle size, zeta potential, transmission electron microscopy, differential scanning calorimetry, rheological behavior and *in vitro* drug release. A stability study for 6 months was performed. A microbiological study was conducted in male rats infected with *Candida albicans*, by counting the colonies and examining the histopathological changes induced on the skin of infected rats. The results showed that SLNs dispersions are spherical in shape with particle size ranging from 83.26±11.33 to 955.04±1.09 nm. The entrapment efficiencies are ranging from 19.73±1.21 to 72.46±0.66% with zeta potential ranging from -18.9 to -38.8 mV and shear-thinning rheological Behavior. The stability studies done for 6 months showed that nystatin (Nyst) is a good candidate for topical SLN formulations. A least number of colony forming unit/ ml (cfu/ml) was recorded for the selected NystSLN compared to the drug solution and the commercial Nystatin® cream present in the market. It can be fulfilled from this work that SLNs provide a good skin targeting effect and may represent promising carrier for topical delivery of Nyst offering the sustained release and maintaining the localized effect, resulting in an effective treatment of cutaneous fungal infection.

***Keywords*—**Candida infections, Hot homogenization, Nystatin, Solid lipid nanoparticles, Stability, Topical delivery.

I. Introduction

SOLID lipid nanoparticles (SLNs), had attracted attention as a drug delivery system since it was introduced in 1991[1].

SLNs are in the submicron size range of 50-1000 nm and are composed of physiologically tolerated lipid components which are in solid state at room temperature.

SLNs are referred to as alternative carrier system to traditional colloidal system such as liposomes, emulsions and polymeric nanoparticles due to its exceptional stability, scaling-up potential and biocompatible components [2].

Nystatin (Nyst) is a polyene antibiotic produced by *Streptomyces noursei*; used topically in treatment of infections due to *Candida albicans*, *Aspergillus* species, yeasts and some dermatophytes. It is often used in large doses which vary from 100,000 units (for oral infections) and 1 million (for intestinal ones) Nystatin is often used as prophylaxis in patients who are at risk of fungal infections such as AIDS patients and patients receiving chemotherapy. Trials to improve the effectiveness of Nyst or decrease its dose are ongoing. Recently, topical formulation of Nyst was developed, Quinones et al, prepared a Nyst gel for topical delivery [3].The aim of the current study is to develop lipid nanoparticulate formulations of Nyst in an attempt to increase its efficacy for topical application. Its formulation in solid lipid nanoparticles may promote its lethal effect as its mode of action depends on its binding to ergosterol, a major component of the fungal cell membrane forming pores in the membrane that lead to potassium leakage and death of the fungus.

II. Materials and Methods

A. Materials

Nystatin, was kindly supplied by Rameda Pharmaceuticals, Sixth of October, Egypt. Compritol 888 ATO (glyceryl behenate) was kindly donated by Gattefossé, France. Poloxamer 188 (Pluronic F68; a triblock copolymer of polyoxyethylene-polyoxypropylene), PVA (polyvinyl alcohol), Dialysis tubing cellulose membrane (molecular weight cut-off 12,000-14,000 g/mole) and Methanol were purchased from Sigma-Aldrich Chemical Company., St.louis, USA. Potassium dihydrogen orthophosphate and citric acid were of analytical grade.

B. Formulation Technique

Solid lipid nanoparticles were prepared by the modified high shear homogenization and ultrasonication method [4]-[6]. The lipid was melted to approximately 5ºC above its melting point (74.09ºC); Nyst was dispersed in the melted Compritol 888 ATO. An aqueous phase was prepared by dissolving the surfactant (poloxamer 188 or PVA) in distilled water and heating up to the same temperature of the molten lipid. The hot lipid phase was poured on the aqueous phase and homogenization was carried out at 25000 rpm for 5 minutes using Heidolph homogenizer. The resulted O/W emulsion was

R.M., M.A., M.S., and M.M. are with the department of pharmaceutical Technology, National Research Centre, Giza, Egypt (e-mail: rawia_khalil@yahoo.com).

A.A. is with the Department of Pharmaceutics, Faculty of pharmacy, Cairo University.

G.A. is with Chemistry of Natural and Microbial Product Department, National Research Centre, Dokki, Cairo, Egypt.

S.S. is with Electron Microscopy Research department Theodor bilharz Research Institute, Cairo, Egypt.

Open Science Index, Pharmacological and Pharmaceutical Sciences Vol:8, No:7, 2014 publications.waset.org/9999007.pdf

sonicated for 30 minutes (water bath sonicator). The dispersion thus obtained was allowed to cool to room temperature, forming lipid nanoparticles by recrystallization of the dispersed lipid [7]. The produced NystSLNs were kept at 4ºC for 24 hours before centrifugation at 9000 rpm for 30 minutes and separation. Different formulations are presented in Table I.

TABLE I
COMPOSITION OF NYSTSLNS

Formulations	Surfactant		Lipid concentration (%w/w)	Drug concentration (%w/w)
	Type	Conc.		
SLN1	Poloxamer 188	1	5	0.25
SLN2		2.5		0.125
SLN3		2.5		0.25
SLN4		2.5		0.5
SLN5		5		0.25
SLN6		2.5	7.5	0.25
SLN7		2.5	10	0.25
SLN8	PVA	1	5	0.25
SLN9		2.5		0.125
SLN10		2.5		0.25
SLN11		2.5		0.5
SLN12		5		0.25
SLN13		2.5	7.5	0.25
SLN14		2.5	10	0.25

III. CHARACTERIZATION

A. Particle Size and Zeta potential Measurement

Size and zeta potential of SLN were measured using a Zetasizer (Nano ZS) at 25ºC. Samples were diluted appropriately with the aqueous phase of the formulation for the measurements.

B. Entrapment Efficiency Measurements

The entrapment efficiency was determined indirectly by measuring the concentration of the drug in the supernatant after centrifugation. The unentrapped Nyst was determined by adding 1ml of NystSLNs to 9 ml methanol and then this dispersion was centrifuged at 9000 rpm for 30 minutes at -4 ◦C, and then washed 3 times with methanol. The supernatant was collected, filtered through millipore membrane filter (0.2µm) then diluted with methanol and measured spectrophotometrically at λ=303.8 nm. The entrapment efficiency was calculated using the following equation [8], [9]:

$$E.E\% = \frac{W \text{ initial drug} - W \text{ free drug} \times 100}{W \text{ initial drug}}$$

where "W initial drug" is the mass of initial drug used and the "W free drug" is the mass of free drug detected in the supernatant after centrifugation of the aqueous dispersion.

C. Transmission Electron Microscopy (TEM)

The morphologies of the selected SLNs were examined by TEM. One drop of diluted sample was stained with 2 % (W/V) phosphotungstic acid for 30 seconds and then placed on copper grids with films for viewing.

D. pH Measurements

The pH values of the prepared lipid nanoparticles were measured using digital pH meter at 25 ºC, the pH meter was previously standardized using buffer solution at pH7.0. All measurements were performed in triplicate.

E. Differential Scanning Calorimetry

The thermal characteristics of selected batches of lipid nanoparticles were determined by differential scanning calorimetry (DSC). Samples containing 10 mg nanoparticle dispersions were weighed accurately into standard aluminium pans using an empty pan as a reference. DSC scans were recorded at a heating and cooling rate of 10 ºC/min. The samples were heated from 30 to 300 ºC and cooled from 300 to30 ºC under liquid nitrogen.

F. Rheological Studies

The rheological measurements were carried out to study the flow curves of different lipid nanoparticles. All measurements were performed at a temperature of 25±0.1°C using a computerized rheometer equipped with a cone and plate geometry (plate diameter 40 mm, cone angle 4^o). For each sample continuous variation of the speed rate from 1 to 100 s^{-1} then backward from 100 to 1 s^{-1} was applied and the resulting viscosity was measured.

IV. DRUG RELEASE STUDY

The *in vitro* release of Nyst from different SLNs was evaluated by the dialysis bag diffusion technique reported by Yang, et al [10]. The release studies of Nyst from lipid nanoparticles were performed in phosphate buffer of pH5.5 and methanol (70:30). NystSLNs equivalent to 2 mg of Nyst were suspended in the buffer solution (ph 5.5) and placed in a dialysis bag (donor compartment) and sealed at both ends. The dialysis bag was immersed in the receptor compartment containing 50ml of dissolution medium, which was stirred at 100 rpm and maintained at 32±2ºC. The receptor compartment was covered to prevent evaporation of the dissolution medium. Samples (2 ml) were taken from the receptor compartment and the same amount of fresh dissolution medium was added to keep a constant volume at fixed time intervals (0.5, 1, 2,3,4,5,6,7,8 and 24 h). Nyst in the samples was measured spectrophotometrically at λ=305.4 nm. The release studies were carried out in triplicate for all formulations and the results were expressed as the mean values ±SD.

V. STABILITY STUDY

The selected SLN formulations were stored in a sealed amber colored glass vials at refrigerator temperature (2-4°C) in a dark environment. The physical appearance was assessed and the formulations were analyzed with respect to particle size, drug entrapment efficiency and zeta potential after 6 months of storage and compared with fresh formulations. In addition, the drug release study of the NystSLNs stored for 6

Open Science Index, Pharmacological and Pharmaceutical Sciences Vol:8, No:7, 2014 publications.waset.org/9999007.pdf

months was performed and compared with fresh formulations. The experiment was performed in triplicate. Shelf life values were calculated as follows [11]

The values of Log (E.E. %) were plotted against the time (days of storage) and the slopes (m) were calculated by linear regression. The slopes (m) were then substituted into the following equation for the determination of K values [12]: K= m x 2.303.

As reported by Wells [13], the shelf life values (the time for 10% loss, t_{90}) were then calculated by the following equation: t_{90} =0.105/K.

VI. Antifungal Activity

A. Preparation of the Animals

Male albino rats (120-150g) purchased from the animal house of the National Research Centre was used in the experiment. The experimental animals were divided into 4groups each containing 6 animals. Group 1 served as control, group 2 was treated with plain drug solution, and group 3 received topically an equivalent dose of Nystatin® cream as a reference. Group 4 was treated with SLN2 formula. The rats were housed in individual cages and received food and water *ad libitum*. The experimental protocol of the study was reviewed and approved by the Animal Ethics Committee of the National Research Centre. Experiments were carried out in accordance with the guidelines laid down by the National Research Centre regarding the care and use of animals for experimental procedures and in accordance with local laws and regulations.

B. Preparation of Microorganism

Clinical isolate of *Candida albicans was* used to infect the animals. A working culture of *Candida* was grown for 24h at 37°C on Potato Dextrose Broth (PDB). The culture was diluted with a sterile saline solution to reach to a final concentration of 1.1 $X10^6$ colony forming unit/ ml (cfu/ml) according to the modified method of Maebashi et al., 1995[14].

C. Cutaneous Infection

Each animal's back was shaved; approximately 5.0cm^2 areas was marked on each animal's back. The marked area was infected with 1.1 $X10^6$ cfu/ml suspension by gently rubbing onto the skin with the help of a sterile cotton-tipped swab until no more visible fluid was observed [14] .Infection was produced under an occlusive dressing and the infected area was covered with a sterile adhesive bandage, held in place with extra-adherent tape for 24h before treatment began. Control animals were infected in the same manner; however, they did not receive any Nyst formulation.

D. Treatment of the Infection

Treatment began 24h after the infection was induced, and test formulations were topically applied twice daily for two consecutive days. After 48 h of treatment swabs were taken from each infected area into sterile tubes containing 5 ml of (PDB). Serial dilutions were done and then one ml of each dilution was inoculated into Petri dishes containing 10 ml of Potato Dextrose Agar (PDA) .The inoculated plates were incubated for 24h at 37˚C after which the colonies were counted.

E. Histopathological Examination

After taking the skin swab in a way the skin is completely cleaned out from the infected organism, the rats are sacrificed. The defined part of the shaved skin is excised and fixed in 10% formalin. The fixed skin tissues were processed until embedded in paraffin [15].Two sections of 4µm thickness were performed from each skin embedded in paraffin block using microtome. One section was stained with Haematoxylin and eosin as well as the other was stained with Masson trichrome [15].

F. Statistical Analysis

All experiments were repeated three times, and data were expressed as mean values. The statistical analysis was carried out using one-way analysis of variance. A P value of less than 0.05 was considered statistically significant.

VII. Results and Discussion

A. Particle Size

Particle size of the nanoparticles is presented in Table II. Particle size measurement was required to confirm the production of the particles in nano-range. The results indicate that particle size was influenced by most of the formulation variables. Among the two surfactants tested, there was a gradual decrease in particle size with an increase in surfactant concentrations (SC) (Table II). This observation was noticed for all formulations except for SLN12, where an increase in the surfactant concentration from 2.5 to 5%w/w causes an increase in particle size. The decrease in nanoparticales size at high surfactant concentration is due to effective reduction in interfacial tension between the aqueous and lipid phase leads to the formation of emulsion droplets of smaller size. Additionally, enough surfactant was present to cover the tiny lipid droplets' surface at higher surfactant concentration, which stabilize and prevented the coalescence of the nanoemulsion droplets [16]. It is evident from the above data that using PVA gave rise to nanoparticles of larger size compared to those using poloxamer 188. Compritol concentration also affects the size as shown in Table II, the particle size significantly increased with increasing lipid concentration (LC). It was noticeable that SLN6, SLN7, SLN13 & SLN14 show larger particle size at 7.5% (w/w) and 10% (w/w) compritol concentrations. The increase in particle size with increasing compritol concentration could be explained by the fact that homogenization efficiency decreases with increasing content of dispersed phase (lipid phase) [17]. Furthermore, the high viscosity and low limiting concentration for lipid aggregation at the interface will cause a decrease of solvent diffusion and hence fewer lipid molecules will be carried into the aqueous phase. Therefore, the formation and stabilization of small lipid aggregates at these concentrations 7.5%w/w and 10%w/w are reduced [18]. The drug

Open Science Index, Pharmacological and Pharmaceutical Sciences Vol:8, No:7, 2014 publications.waset.org/9999007.pdf

concentration has also a marked role on the particle size. The results show that the particle size increases with increasing drug concentration (DC) from 0.125 %(w/w) to 0.5%(w/w) (Table II).This can be explained as before: the lipid has a certain loading capacity, the addition of excess drug may lead merely to the formation of large sized particles.

B. Zeta Potential

As depicted in Table II, all formulations were negatively charged, the zeta potential varies from -18mV for SLN2 to -38.8mV for SLN12 indicating a relatively good stability and dispersion quality. It was noticeable that as the amount of surfactant increased in the formulation, the zeta potential became more negative. However, the influence of surfactant type is less pronounced. Considering the effect of lipid concentration (compritol), as lipid concentration increased the zeta potential was found to be more negative (Table II). Other researchers also noticed the same observation when studying the effect of increasing compritol amount in the final formulation [17], [19].

C. Drug Entrapment Efficiency

Increasing surfactant concentrations from 1 to 5% w/w in presence of 5% w/w compritol and 0.25% w/w nystatin was accompanied with increase in the E.E.%, (SLN1, SLN3 &SLN5) and (SLN8, SLN10 & SLN12) for poloxamer 188 and PVA respectively (Table II) . The possible reason for this observed increase in the E.E% might be due to sufficient covering of the lipid core so as to minimize possible leaching of the drug by preventing drug diffusion to the external phase of the medium [20]. This increase in the E.E% may be also due to the increase in the solubility of the drug in the lipid on increasing the concentration of the surfactant [16], [21]. On the other hand, the influence of surfactant type is not well-defined on the entrapment efficiency. As expected, Table II shows that upon increasing the concentration of compritol while keeping the concentration of surfactant at 2.5 % w/w and Nyst at 0.25% w/w, a gradual increase in the entrapment efficiencies of NystSLNs in case of poloxamer 188(SLN3, SLN6 & SLN7) & PVA (SLN10, SLN13 & SLN14) was observed . A possible explanation for this observation is that the increase in lipid content can afford more space to encapsulate more drugs and thus reduces the drug partition in the outer phase[22].Increasing the amount of drug, while keeping the emulsifier level constant, as shown in Table II, is found to decrease the E.E%. As the lipid has certain drug loading capacity, addition of excess drug led to increase of unencapsulated drug (i.e. decrease in E.E.%), which signifies that E.E.% reaches its maximum point at 0.125% drug concentration [23].

TABLE II
ENTRAPMENT EFFICIENCY (E.E.), PARTICLE SIZE (PS), ZETA POTENTIAL (ZP) OF NYSTSLNS.

Formulations	E.E (%)	P.S(nm)	ZP(-mv)
SLN1	19.73±1.21	196.19±7.51	20.2
SLN2	56.83±3.21	123.75±25.52	18.9
SLN3	27.97±1.60	190.10±2.30	21.5
SLN4	28.91±2.81	333.50±2.12	25.9
SLN5	64.35±1.71	83.26±11.33	23.2
SLN6	37.22±1.40	210.10±17.28	26.4
SLN7	44.95±2.01	318.65±33.02	29.9
SLN8	38.19±1.06	615.10±0.00	23.6
SLN9	56.48±4.01	164.20±25.23	21.4
SLN10	43.79±2.34	607.05±11.38	26.5
SLN11	35.14±1.74	458.70±0.00	29.2
SLN12	72.46±0.66	712.40±22.70	38.8
SLN13	44.82±2.96	955.20±2.77	26.8
SLN14	53.23±3.95	955.40±1.09	26.3

D. Transmission Electron Microscopy

Transmission electron micrographs indicate that the prepared SLNs have a nanometer-size with no drug crystal formation. Most of the particles were round and uniform in size with smooth surface morphology (Fig. 1).

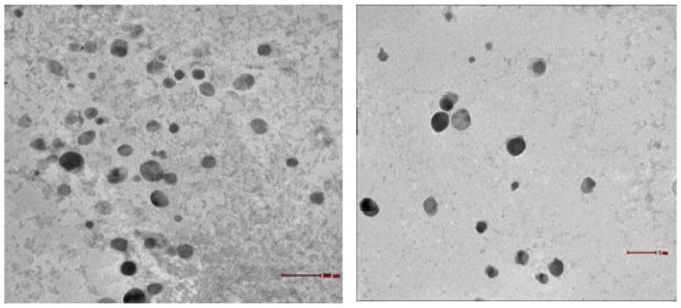

(a) (b)

Fig. 1 Transmission electron micrographs of different SLN formulations (a) SLN2, (b) SLN9

E. pH Measurement

The bulk pH of the stratum corneum and upper viable epidermis have been measured and found to be 4.0-4.5 and 5.0-7.0, respectively [24]. For a topical preparation to be applied safely to the skin, its pH should lie within this range. The pH of different NystSLNs formulations ranges from 5.25±0.028 to 6.14±0.007. These results are within the required range.

F. Differential Scanning Calorimetry

Thermal behavior of the pure drug, as well as of compritol compared with the thermograms of different lyophilized SLNs formulae in the range of 30-300°C is shown in Fig. 2. Crystalline Nyst demonstrates a sharp endothermic peak at 167.11°C corresponding to its melting temperature. While a sharp endothermic peak at 74°C was observed for compritol. Absence of the peak at 167.11°C in NystSLNs (SLN2 & SLN9) indicates either formation of amorphous dispersion of Nyst in the lipid matrix or solubilization of Nyst in the lipid matrix upon heating. Similar results were obtained by Das et

Open Science Index, Pharmacological and Pharmaceutical Sciences Vol:8, No:7, 2014 publications.waset.org/9999007.pdf

al. in studying the thermal analysis of tretinoin loaded SLNs and proving the amorphous dispersion and solubilization of tretinoin upon heating [25]. Nystatin loaded SLNs show a broad endothermic peak at approximately 72ºC. This slight shift in the endothermic peak of compritol is probably due to drug loading in lipid matrix

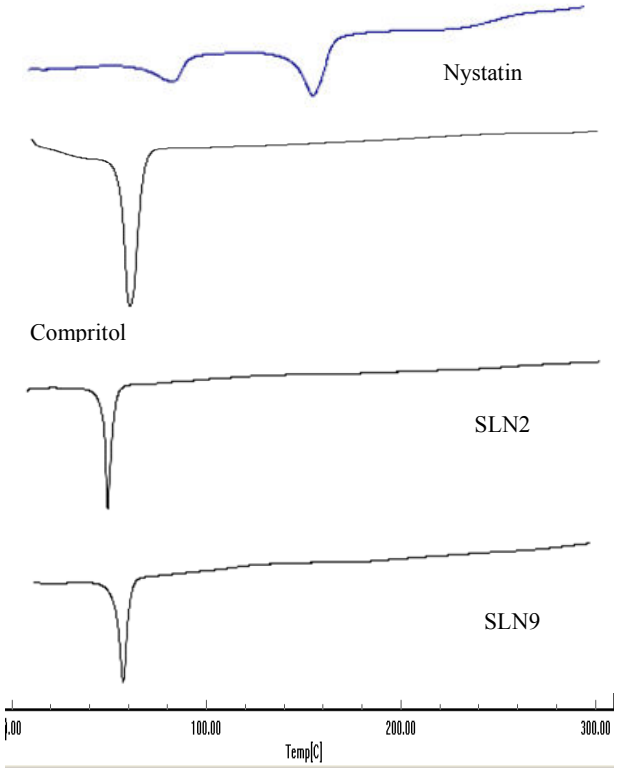

Fig. 2 DSC thermograms of pure Nyst, bulk compritol lipid and different SLN formulations

G. Rheological Study

The rheological properties of SLN formulations were presented by plotting the shear stress versus the shear rate (flow curve) and the viscosity against the shear rate (viscosity curve) [26], [27]. The rheograms of selected SLN formulations are shown in Fig. 3. As shown from the figure, SLN dispersions revealed a non-Newtonian pseudo plastic flow described by a shear thinning where the viscosity of the dispersions decreases with increasing the shear rate which is a good characteristic in pharmaceutical preparations for topical application. When the preparation is subjected to shear force, its network structures break down leading to a gradual decrease in the viscosity in order to spread on the skin. When the shear force is removed, the viscosity is recovered and the increased viscosity keeps the preparation on the skin.

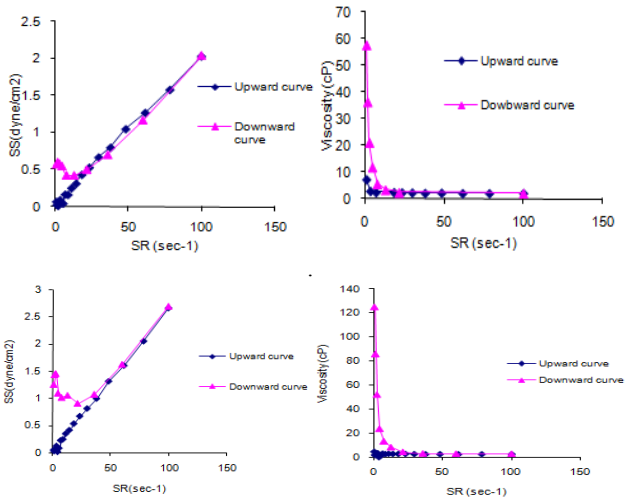

Fig. 3 Rheograms of NystSLN2 and NystSLN9

H. Drug Release Study

The data clearly show that the release of the drug can be influenced by the type and concentration of surfactant and the concentration of Nyst (Fig. 4). Formulae SLN1, SLN3 &SLN5 as well as SLN8, SLN10 & SLN12 show that upon increasing the concentration of surfactants, the release efficiency decrease. The decrease in drug release efficiency at higher surfactant concentrations is most likely due to retardation of the drug release caused by micellar entrapment of the drug. The slow release of Nyst from all the formulae suggests homogenous entrapment of the drug throughout the systems [28]. Nyst is released more quickly when used in lower concentrations (SLN2, SLN3, SLN4 & SLN9, SLN10, SLN11) because of the drug-enriched shell model [29], [30]. According to this model, a solid lipid core forms when the recrystallization temperature of the lipid is reached. On reducing the temperature of the dispersion, the drug concentrates in the still liquid outer shell of the SLN (Fig. 5). Fig. 6 shows that the increase in the lipid concentration is accompanied with a decrease of the percentage of Nyst released (SLN3, SLN6, SLN7, SLN10, SLN13 and SLN14). This decrease can be attributed to the higher lipid content encapsulating the drug which may increase the diffusion distance for drug to diffuse out from the Solid Lipid Nanoparticles [31].

Open Science Index, Pharmacological and Pharmaceutical Sciences Vol:8, No:7, 2014 publications.waset.org/9999007.pdf

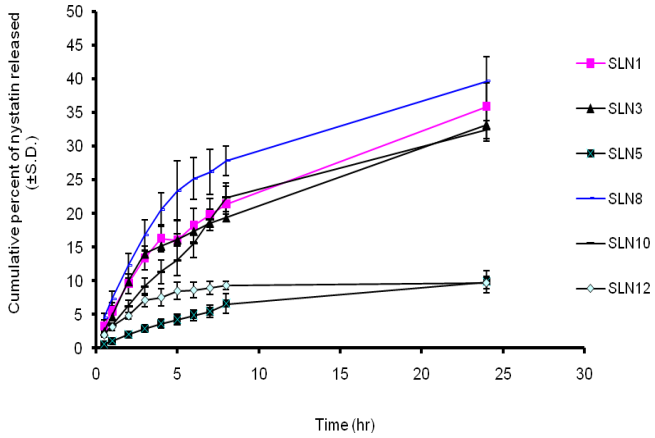

Fig. 4 Effect of types and concentrations of surfactant on the *in vitro* release of Nyst from SLNs

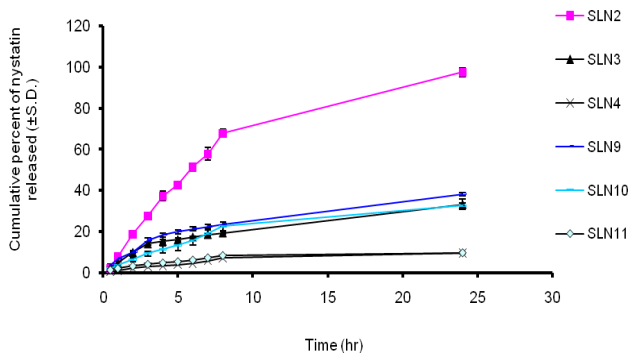

Fig. 5 Effect of drug concentration on the *in vitro* release of Nyst from SLNs

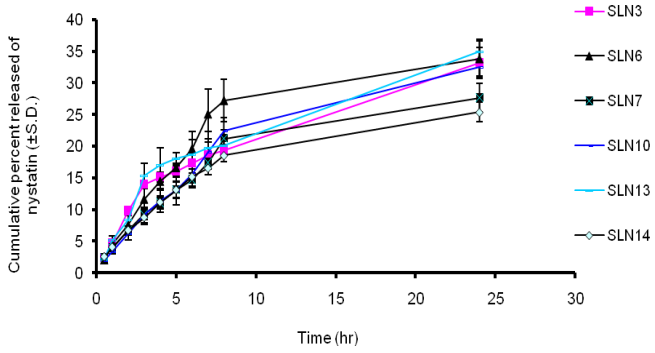

Fig. 6 Effect of lipid concentrations on the *in vitro* release of Nyst from SLNs

I. Stability Studies

The stability study was carried out for 2 formulations: SLN2 and SLN9 as they show the highest cumulative percent of Nyst released. NystSLNs formulations didn't show visual physical instability up to a period of 6 months. Table III shows that the NystSLNs showed minor enhancement of particle size, zeta potential and entrapment efficiency in case of SLN2. However, the changes in E.E. % were insignificant. Although sustained drug release was observed from both formulations after 6 months of storage, the release was relatively faster from stored SLNs than from fresh ones (Fig. 7). This faster release in case of SLN9 compared to SLN2 might be due to rearrangement of crystal lattice in the SLN lipid matrix over time, which pushes some of the drug molecules to migrate towards the nanoparticle surface [25]. Table IV reports the entrapment efficiency of the different formulations as a function of time. Shelf life value (t_{90}) i.e., the time at which the drug concentration has lost 10% was calculated and reported also in Table IV. The results revealed that SLN2 and SLN9 could maintain 90% of Nyst stability for more than 9 and 3 months respectively. In this respect it can be hypothesized that the stability of Nyst is better controlled in SLN2.

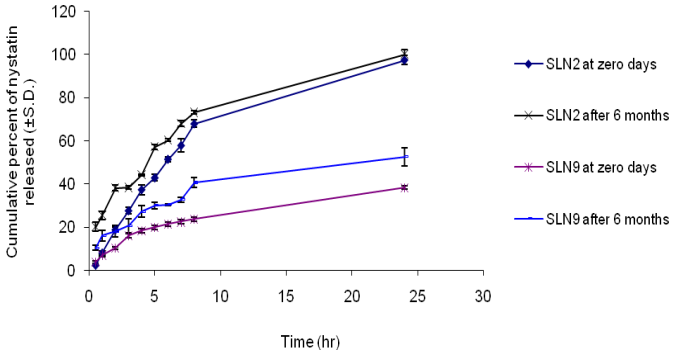

Fig. 7 Effect of storage time on the *in vitro* release of Nyst from SLNs

TABLE III
STABILITY PROFILE OF NYSTSLNS

Items for comparison	Formulations	
	SLN2	SLN9
Entrapment efficiency		
Fresh	56.58±3.21	58.77±4.01
After 6 months	52.23±1.25	47.33±1.32
Particle size		
Fresh	123.75±25.52	164.2±25.23
After 6 months	160.1±13.60	218.2±4.80
Zeta potential		
Fresh	-18.9	-21.4
After 6 months	-27.7	-34.1

TABLE IV
NYSTSLNS ENTRAPMENT EFFICIENCY AS A FUNCTION OF TIME

Time	Entrapment efficiency(E.E.%)	
	SLN2	SLN9
0	56.58±3.21	58.77±4.01
2	54.62±2.10	56.77±3.11
4	54.02±0.77	56.80±1.22
6	52.23±1.25	47.33±1.32
K	0.011	0.032
t_{90} (months)	9.13	3.28

* Where K is the stability constant =slope x 2.303
* t_{90} is the time at which the drug concentration has lost 10% = 0.105/K

I. Antifungal Activity

After two days of treatment with plain drug solution, commercial Nystatin® cream and the tested formula (SLN2) (Table I), the animals treated with SLN2 demonstrated a low colony count and the number of colony forming unit/ ml

Open Science Index, Pharmacological and Pharmaceutical Sciences Vol:8, No:7, 2014 publications.waset.org/9999007.pdf

(cfu/ml) recorded for the selected formula (SLN2) was significantly ($p \square 0.05$) less than that for those animals treated with plain drug solution and commercial Nystatin® cream (Fig. 8). On the other hand, the animals treated with the Nystatin® cream show no significant difference ($p>0.05$) with those treated with the plain drug solution/. The higher therapeutic efficacy in the case of SLN formulation may be due to their lipid nature and structural integrity as nanoparticles might be the causal factor for more prolonged and significantly enhanced antifungal activity [32],[33]. These findings also confirmed that lipid nanoparticles provoke the accumulation of the embedded drug into the upper skin layers [34].

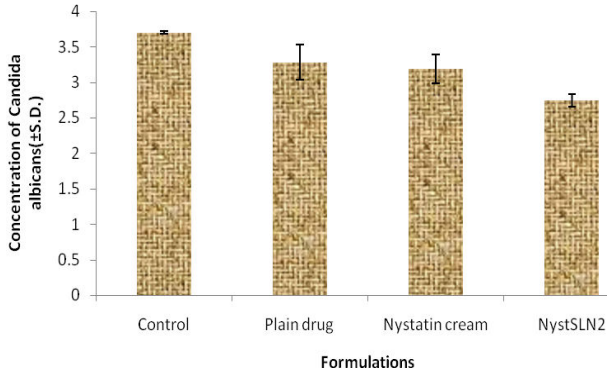

Fig. 8 Antifungal efficacy of Nystatin formulations expressed as cfu after treatment.

It is clear from the histopathology (Figs. 9-13) of the skin biopsies stained with Masson trichrome & Haematoxylin and eosin that the skin of the normal control rat reveals keratinized squamous epithelium with intact basal cell layer and basal lamina (Fig. 9). The basal part of the epidermis is folded to form the dermal papillae. Hair follicles were clearly identified with their different constituents extending into the dermis. The dermis formed the thick connective tissue layer in which the hair follicles were seen with sebaceous glands. These histological findings agree with the previously reported data in the literature containing the constituent of normal skin [35]. However, Masson trichrome stained skin of *Candida albicans* infected control rat reveals erosion or ulceration of the epidermis, edematous dermis and increased dermal vascularities. Also complete loss of the hair follicles with apparent sweat glands is observed (Fig. 10). Masson trichrome and Haematoxylin stained skin sections of rat infected with *Candida albicans* and treated with the available drug solution (Fig. 11) or the commercial Nystatin® cream formula present in the market (Fig. 12), reveals a smaller area of skin erosion, minimal ulceration and no characteristic hair follicles.

The effect of SLN2 formula was comparable to the effect of the drug solution or the commercial Nystatin® cream with the advantage of the appearance of few primitive hair follicles in the upper part of the dermis and mild polymorphnuclear leucocytes infiltrate (Fig. 13).

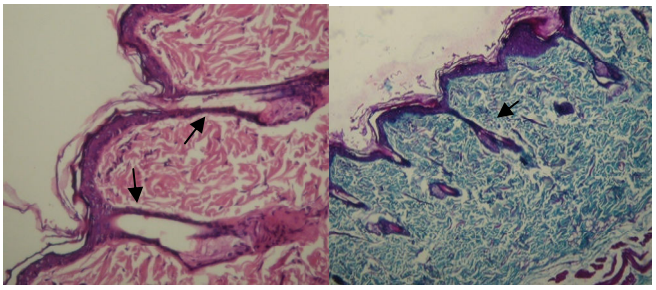

(a) (b)

Fig. 9 (a) and (b) show normal skin stained with Hamatoxylin & eosin and Masson Trichrome respectively. Both sections reveal intact keratinized epidermis. The hair follicles (arrow) extend from the epidermis down into the dermis. Notice the thick dermal layer.

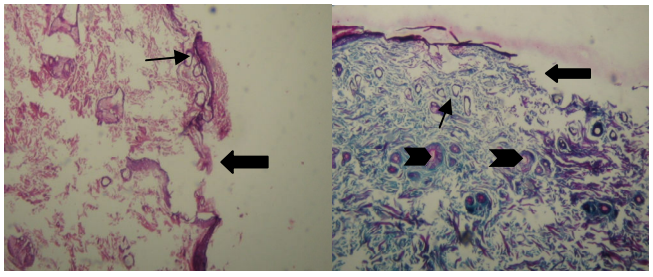

(a) (b)

Fig. 10 Haematoxylin & eosin (a) and Masson trichrome (b) stained skin sections for control rat infected with Candida albicans reveal discontinuous ulcerated epidermis (thick arrow) in the vicinity of incomplete loss of other part or erosion. Many new vessels formation are disclosed in the upper part of the dermis (thin arrows). Note the absence of hair follicles and increased sweat glands (head of arrow) in the dermis. (x100)

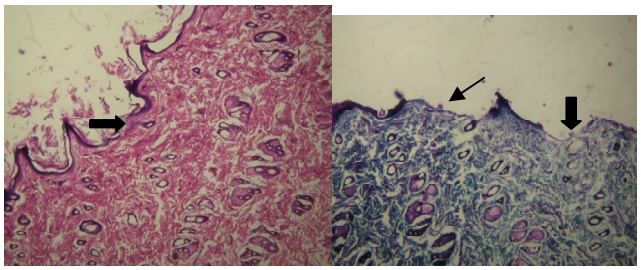

(a) (b)

Fig. 11 Photomicrographs showing sections of rats skin treated with plain drug solution, (a) section stained with Haematoxylin and Eosin, (b) section stained with Masson trichrome. The sections reveal area of skin erosion (arrow), minimal ulceration (thick arrow) and no characteristic hair follicles

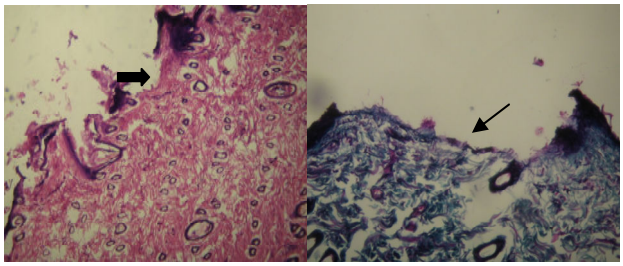

(a) (b)

Fig. 12 Photomicrographs showing sections of rat's skin treated with Nystatin® cream, (a) section stained with Haematoxylin and Eosin, (b) section stained with Masson trichrome. The sections reveal area of skin erosion (arrow), minimal ulceration (thick arrow) and no characteristic hair follicles

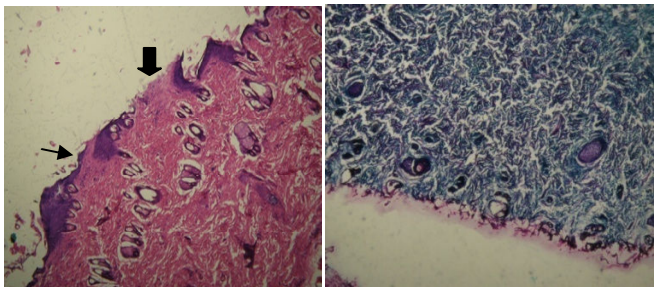

(a) (b)

Fig. 13 Photomicrographs showing sections of the rat skin treated with NystSLN2, (a) section stained with Haematoxylin and Eosin, (b) section stained with Masson trichrome. The sections reveal areas of erosion (thin arrow) and ulceration (thick arrow). Note the appearance of primitive hair follicles in the subepidemal area (black arrows) and mild polymorphnuclear leucocytes infiltration

VIII. Conclusion

Homogenization followed by ultrasonication method is suitable to produce NystSLNs with small-size particles (nanosize) and shear-thinning rheological behavior. The loading of Nyst proved to follow the drug-enriched-shell theory. DSC analysis showed amorphous state of Nyst. The *in vitro* release behavior was greatly affected and can be controlled by optimizing the formulation variables. Stability studies proved that the 2 formulae suggested SLN2 and SLN9 are stable upon storage could maintain 90% of Nyst stability for more than 9 and 3 months respectively. NystSLN2 formula tested for antifungal activity showed better results compared to the drug solution and the commercial Nystatin® cream.

References

[1] Muller RH, Mader K, Gohla S, Solid lipid nanoparticles (SLN) for controlled drug delivery- A review of the state of the art. Eur J Pharm Biopharm 2000; 50: 161-177.
[2] Radomska-Soukharev A, Stability of lipid excipients in solid lipid nanoparticles. Adv Drug Deli Rev 2007; 59: 411-418.
[3] Quinones D, Evone MS, Ghaly S, Formulation and characterization of nystatin gel. PRHSJ 2008; 27: 62.
[4] Sandri G, Bonferoni MC, Gokce EH, Ferrari F, Rossi S, Patrini M, Caramella C, Chitosan associated SLN: *in vitro* and *ex vivo* characterization of cyclosporine A loaded ophthalmic systems. J Of Microencapsulation 2010; 27: 735-746.
[5] Sharma A, Jindal M, Aggarwal G, Jain S, and Development of a novel method for fabrication of solid lipid nanoparticles: using high shear homogenization and ultrasonication. RJPBCS 2010; 1: 266.
[6] Ekambaram PA, Abdul Hassan Sathali K, Priyanka, Solid lipid nanoparticles: A review. Scientific Reviews & Chemical Communications 2012; 2: 82-85.
[7] Gohla SH, Dingler A, Scaling up feasibility of the production of solid lipid nanoparticles (SLN). Pharmazie 2001; 56: 61-63.
[8] Souto EB, Wissing SA, Barbosa CM, Muller RH, Development of a controlled release formulation based on SLN and NLC for topical clotrimazole delivery. Int J Pharm 2004; 278:71.
[9] Jifu H, Xinsheng F, Yanfang Z, Jianzhu W, Fengguang G, Fei L, Xinsheng P, Development and optimization of solid lipid nanoparticle formulation for ophthalmic delivery of chloramphenicol using a Box-Behnken design. International journal of nanomedecine 2011; 6: 683-692.
[10] Yang SC, Lu LF, Cai Y, Zhu JB, Liang BW, Yang CZ, Body distribution in mice of intravenously injected camptothecin solid lipid nanoparticles and targeting effect on brain. J Control Release 1999; 59:299.
[11] Esposito E, Bortolotti F, Menegatti E, Cortesi R, Amphiphilic association systems for amphoterecin B delivery. Int J Pharm 2003; 260:249-260.
[12] Ferrer J. Vaginal candidosis: epidemiological and etiological factors. Int J Gynaecol Obstet 2000; 71:21-27.
[13] Wells JI. Pharmaceutical formulations: The physicochemical properties of drug substances. England: Ellis Hortwood, Chichester, 1988:
[14] Maebashi K, Toyama T, Uchida K, Yamaguchi H, A novel model of cutaneous candidiasis produced in prednisolone treated guinea pigs. J Med Vet Mycol. 1995; 19:390-392.
[15] Masson P, Some histological methods. Trichrome staining and their preliminary technique. Bulletin of the International Association of Medicine. 1929; 12: 75.
[16] Abdelbary G, Fahmy RH, Diazepam loaded solid lipid nanoparticles: design and characterization. AAPS Pharm Sci Tech 2009; 10: 215.
[17] Vijayan V, Srinivasa D, Jayachandran E, Anburaj J, Preparation and characterization of anti diabetic drug loaded solid lipid nanoparticles. JITPS 2010; 8: 324.
[18] Quintanar-Guerrero D, Allemann E, Fessi H, Doelker E, Pseudolatex preparation using a novel emulsion-diffusion process involving direct displacement of partially water-miscible solvents by distillation. Int J Pharm 1999; 188: 155-164.
[19] Rahman Z, Zidan AS, Khan MA, Non destructive methods of characterization of risperidone solid lipid nanoparticles. Eur J Pharm Sci 2010; 76: 127-137.
[20] Yang Y, Chung T, Bai X, Chan W, Effect of preparation conditions on morphology and release profiles of biodegradable polymeric microspheres containing protein fabricated by double emulsion method. Chem Eng Sci 2000; 55: 2223-2236.
[21] Ekambaram, P. and Hasan, S.A. Formulation and evaluation of solid lipid nanoparticles of ramipril. J. Young Pharm., 2011; 3:216-220.
[22] Jifu H, Xinsheng F, Yanfang Z, Jianzhu W, Fengguang G, Fei L, and Xinsheng P, Development and optimization of solid lipid nanoparticle formulation for ophthalmic delivery of chloramphenicol using a box-Behnken design. Int J Nanomedicine 2011; 6:687.
[23] Das S, Ng WK, Tan RBH, Are nanostructured lipid carriers (NLCs) better than solid lipid nanoparticles (SLNs): Development, characterizations and comparative evaluations of clotrimazole-loaded SLNs and NLCs? Europ J Pharm Sci. 2012; 47: 139-151.
[24] Plasencia, I., Norlen, L. and Bagatolli, L.A. Direct visualization of lipid domains in human skin stratum corneum's lipid membranes: Effect of pH and temperature. Biophys. J.2007; 93, 3142-3155.
[25] Das S, Ng WK, Kanaujia P, kim S, Tan RB, Formulation design, preparation and physicochemical characterizations of solid lipid nanoparticles containing a hydrophobic drug: effects of process variables. Colloids Surf B Biointerfaces 2011;88:483-489
[26] Illing, A. and Unruh, T. Investigation on the flow behavior of dispersions of solid triglyceride nanoparticles. Int.J.Pharm.2004; 284,123-131.
[27] Liu J., Gong, T., Fu, H., Wang, C., Wang, X., Chen, Q., Zhang, Q., He, Q. and Zhang, Z. Solid lipid nanoparticles for pulmonary delivery of insulin. Int.J.Pharm.2008; 356, 333-344.

Open Science Index, Pharmacological and Pharmaceutical Sciences Vol:8, No:7, 2014 publications.waset.org/9999007.pdf

[28] Venkateswarlu, V. and Manjunath, K. Preparation, characterization and in vitro release kinetics of clozapine solid lipid nanoparticles. J. Control. Release, (2004), 95,627-638.
[29] Heiati H , Tawashi R, Shivers RR, Solid lipid nanoparticles as drug carriers I. Incorporation and retention of the lipophilic prodrug 3'- azido-3'deaxythymidine palmitate. Int J Pharm 1997; 146:123-31.
[30] Muller RH, Radtke M, Wissing SA, Solid lipid nanoparticles (SLN) and nanostructured lipid carriers (NLC) in cosmetic and dermatological preparations. Adv Drug Deliv Rev 2002; 1:131-55.
[31] Pravin P, Anil KS, Subhash CD, Vijay KS, Development of solid lipid nanoparticles of lamivudine for brain targeting. Int J Drug Deliv Tech 2009; 1: 36-38.
[32] Fang JY, Fang CL, Liu CH, SU YH, Lipid nanoparticles as vehicles for topical psoralen delivery: solid lipid nanoparticles (SLN) versus nanostructured lipid carriers (NLC). Eur J Pharm Biopharm 2008; 70: 633-640.
[33] Sivaramakrishnan R, Nakamura C, Mehnert W, Korting HC, Kramer KD, Schafer-Korting M, Glucocorticoid entrapment into lipid carriers-characterization by parelectric spectroscopy and influence on dermal uptake. J Control Release. 2004; 97: 493-502.
[34] Gupta M, Vyas SP, Development, characterization and *in vivo* assessment of effective lipid nanoparticles for dermal delivery of fluconazole against cutaneous candidiasis. Chemistry and Physics of Lipids. 2012; 165: 460.
[35] Amany, M.M. Histological and immunohistochemical study on the effect of tretinoin on the skin of adult male albino rt. Egypt.J.Histol.2008; 31:208-219.

Open Science Index, Pharmacological and Pharmaceutical Sciences Vol:8, No:7, 2014 publications.waset.org/9999007.pdf